Synthesized Synchronous Sampling Technique for Differential Bearing Damage Detection

Huageng Luo
Hai Qiu
George Ghanime

GE Global Research Center,
Niskayuna, NY 12309

Melinda Hirz
Geo van der Merwe

GE Aviation,
Evendale, OH 45215

The differential bearing between the low-pressure turbine (LPT) and high-pressure turbine (HPT) shafts is one of the most vulnerable parts in a turbomachinery engine. Unfortunately, it is also one of the most difficult parts to monitor for damage existence signatures, because the signal-to-noise ratio at the normal sensor locations is extremely low. In addition, the speed variations in both the LPT and HPT can further deteriorate the damage signature extracted by conventional analysis methods. In this paper, we developed a "synthesized synchronous sampling" technique to enhance the detection of differential bearing damage signature. Combining this technique together with the conventional acceleration enveloping technique, we are able to detect differential bearing damage at a much earlier stage, thus providing early warnings of the machinery health conditions. [DOI: 10.1115/1.4000092]

1 Introduction

Vibration signatures are probably the earliest symptoms of an abnormality when it comes to bearing and gear condition monitoring. The applications of a vibration based condition monitoring system for rotating machinery have been well documented [1–4]. With better understanding of bearing and gear damage mechanisms [5–8] and the advancement of signal processing and computer technologies [9–13], vibration signature analysis have become one of the most reliable techniques for bearing and gear incipient fault detection.

With respect to bearing damage modeling, McFadden and Smith [5] proposed one of the earliest models on the bearing damage generation mechanism. In the paper, they proposed a model to describe the vibration excited by a single point defect on the inner race of a rolling element bearing under constant radial load. In a following paper, McFadden and Smith [6] extended their model to describe the vibration signature produced by multiple point defects. This model incorporates the effects of bearing geometry, speed, load distribution, transfer function, and the decay of vibration. Su and Lin [8] further extended the work to include damages located at any part of the bearing under various loading conditions. Later on, Su et al. [14] proposed a mathematical model to describe the frequency characteristics of roller bearing vibrations due to surface irregularities.

On the signal processing side, the acceleration enveloping based technique, also known as the high frequency resonance technique [12] or the demodulation analysis [15], has existed for over 30 years. Acceleration envelope signatures are essentially bandpass filtered bearing vibration signals, where the rotating speed related low frequency component (usually large in amplitude) and high frequency noise are removed. The remaining vibration response is the resonance response of the bearing supporting structure subject to bearing defect excitations. Due to damping in the supporting structure, the impulsive response will decay after the excitations. By detecting the envelope of the decayed response, the repetition of the envelope is uniquely associated with bearing damage in the outer race damage, the inner race, or any of the rolling elements.

The synchronous sampling technique is also widely used in gear and bearing damage signature enhancement, especially in varying speed operations. The synchronous sampling technique converts the equal time sampling to the equal shaft circumferential angle sampling, so that the rotor speed dependency is eliminated. This is usually achieved by installing an encoder onto the bearing support, which monitors the shaft operational speed by counting the physical events passing by. The approach on synchronously sampling data is commonly used to carry out time synchronous averaging to enhance a synchronous coherent signal component of the signal and to attenuate both noncoherent and nonsynchronous components to negligible levels [10,11].

There are many tools to enhance the signature of a conventional bearing with one fixed race. However, in the case of a differential bearing, both bearing races are in motion and the race speeds are not precisely controlled during the engine operation. Furthermore, the differential bearing assembly is located between two shafts and is usually buried under other mechanical components that further diminish signatures transmitted to the vibration sensor. Therefore, synchronous sampling is required to extract the inherently small signature. Due to moving races, the installation of an encoder to derive the relative speed is not physically feasible for a differential bearing. Thus, there is no encoder available for synchronous sampling.

In this paper, we will introduce a technique called the synthesized synchronous sampling to address this fault detection problem. Using the synthesized synchronous sampling technique, together with other signature enhancement techniques such as synchronous averaging and acceleration enveloping, we are able to enhance the feature extraction for differential bearings using "external" sensors.

This paper is organized as follows: Sec. 2 introduces the kinematics of the differential bearing feature frequencies and the shaft speeds; this is followed by brief descriptions of the acceleration enveloping technique, synchronous sampling fundamentals, time synchronous averaging techniques. and order analysis. Section 3 contains a detailed description of the procedures of synthesized synchronous sampling and numerical simulations results. In Sec. 4, data from a bearing rig test with seeded differential bearing outer race damage are analyzed and the results are presented. Finally, conclusions from this research are discussed in the Sec. 5.

Manuscript received March 18, 2009; final manuscript received July 30, 2009; published online April 7, 2010. Assoc. Editor: Patrick S. Keogh.

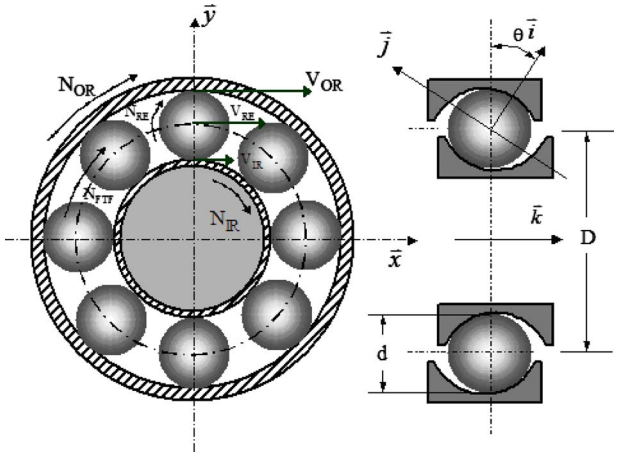

Fig. 1 Ball bearing

2 Fundamentals

2.1 Bearing Kinematics. Rolling element bearings produce vibration excitation forces at specific frequencies dependent on the bearing geometry and rotation speed. These vibration frequencies are called bearing tones. All such bearings, regardless of their condition, will produce some level of bearing tones—the important fact is that their level increases as the bearing deteriorates.

Generally, there are four frequencies associated with a rolling element bearing, as follows:

- Cage frequency or fundamental train frequency (FTF) f_{FTF};
- Rolling element frequency f_{RE};
- Inner raceway frequency f_{BPFI};
- Outer raceway frequency f_{BPFO}.

In many industrial applications, either the outer race or the inner race is fixed and the other raceway is rotating with the shaft. However, in some special cases such as in an aircraft engine application, both the inner and outer raceways may rotate at different speeds.

As shown in Fig. 1, the outer raceway is rotating at speed N_{OR} (in rpm) while the inner raceway is rotating at speed N_{IR} (rpm). In such a case, the bearing frequencies are expressed as

$$f_{FTF} = \frac{1}{120}\left[N_{OR}\left(1 + \frac{d}{D}\cos\,\theta\right) + N_{IR}\left(1 - \frac{d}{D}\cos\,\theta\right)\right] \quad (1)$$

$$f_{RE} = \frac{D}{120d}\left(1 - \frac{d}{D}\cos\,\theta\right)\left(1 + \frac{d}{D}\cos\,\theta\right)|N_{OR} - N_{IR}| \quad (2)$$

$$f_{BPFI} = \frac{n}{120}\left(1 + \frac{d}{D}\cos\,\theta\right)|N_{OR} - N_{IR}| \quad (3)$$

$$f_{BPFO} = \frac{n}{120}\left(1 - \frac{d}{D}\cos\,\theta\right)|N_{OR} - N_{IR}| \quad (4)$$

For a damaged spot on a roller, the fundamental frequency will be $2f_{RE}$, since for each complete rotation of the roller with respect to the cage, the spot will contact the inner and outer races once.

2.2 Acceleration Enveloping. The acceleration enveloping technique was originally called the high frequency resonance technique. It was discovered, almost accidentally, from an oscilloscope display [16] in the early 1970s through a NASA funded project [17]. The acceleration enveloping technique is based on the following assumptions: When a defect occurs in a bearing, repetitive impacts happen during rotation. These kinds of impacts are broadband excitations. These broadband excitations stimulate the resonant response of the bearing supporting system. However, the resonant response levels from the defect impacts are usually very low compared with the shaft excitation such as unbalance, though the frequency contents of the resonant response is usually much higher. If the dynamic range of the vibration sensor and the consequent analyzer is low, the resonant response signals are down in the noise level. The key to detecting bearing faults is to capture the low amplitude response caused by bearing defect excitation without including the high amplitude rotational vibration signals and system fundamental resonant frequency responses. To accomplish this, a bandpass filter is used to isolate the signal. Once the high frequency damage response is captured, the signal goes through a rectification device and the envelope of the signal is detected from the rectified signal. Applying FFT to the envelope signal will reveal the frequency and amplitude, which is uniquely associated with the damaged bearing component.

In theory, any vibration sensor can achieve the bearing damage detection through the enveloping or demodulation processes as long as the sensor has the frequency range required. Since the bearing damage excited response is known to have high frequency content, the accelerometer has an advantage over velocity and displacement sensors.

In the early days, this enveloping detection process was performed using several analog devices. As shown in Fig. 2, the conditioned vibration sensor signal is first passed through an analog filter to isolate the impulse response excited by the bearing damage. The filtered response is then passed through a rectifier to flip the negative half of the oscillation signal to the positive side. The rectified signal is fed into an envelope detector to identify the envelope of the signal. The envelope signal is then used to identify the bearing damage signature through a signal analyzer. If necessary, a low-pass filter can be added before the analyzer.

The process shown in Fig. 2 works well if all the analog devices are appropriately designed for a particular application. However, a different application may require different parameter settings of the analog devices. For example, the bearing support system may have a different resonant structure, thus it requires a different cutoff frequency design for the bandpass filter to isolate the damage impulse response. For different structural dampings, the envelope detector needs a different time constant design to match the impulse response decaying rate, so that those bearing damage related high frequency and low level vibration signals can be maximized. More importantly, the bearing damage detection is usually conducted in a harsh environment. An increase in electronic components involved in the bearing detection process usually decreases the overall system reliability.

With the improvement of computer technology and the development of high dynamic range analog to digital (A/D) converters, the acceleration enveloping based bearing damage detection becomes much easier to implement nowadays. Many of the analog devices, as shown in Fig. 2, can now be replaced by digital signal processing techniques, thus improving the detection accuracy and system reliability. One possible digital signal processing based realization of the acceleration enveloping is shown in Fig. 3. The conditioned acceleration signal is first digitized with the high-speed and high-dynamic range A/D converter. The high-speed and high-dynamic range A/D is especially important because it ensures that the digitized vibration data contain low amplitude, high frequency resonant responses excited by the bearing damage impulse. The digitized data are then passed through a digital bandpass filter to isolate the resonant response excited by the bearing damage. Next, the enveloping detection algorithm is used to detect the envelope of the filtered data. In the digital domain, this process can be achieved by the Hilbert transform. The digital Hilbert transform is related to the FFT and can be easily achieved [18]. If accurate enveloping detection is required, a local maximum interpolation technique can provide better results [19]. The bearing damage detection is then accomplished by spectrum analysis on the enveloped data.

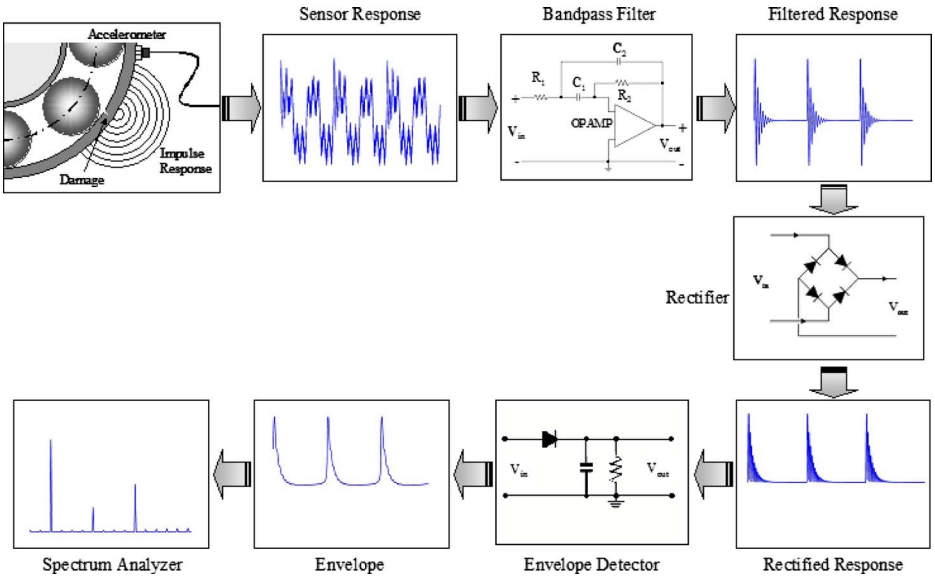

Fig. 2 Analog devices based approach

2.3 Synchronous Sampling and Synchronous Analysis. For rotating machinery, vibrations may occur at multiples and submultiples of the shaft speed. For example, if the shaft is rotating at 3600 rpm, which is 60 Hz, then the vibration response is at multiples of this frequency and sometimes a fraction of this frequency can be seen. These multiples are called the orders (or harmonics in musical terms). The general relationship between the order (O), the shaft speed (RPM), and the frequency (f) in Hz is

$$f = \frac{O \times RPM}{60} \tag{5}$$

If the rotating speed is fixed, a regular FFT analysis can give the desired results. However, if the rotor speed changes within the time window of data acquisition, the variation in the rotor speed will cause the fundamental and harmonics in the frequency domain to be smeared out in the neighborhood. That is why in rotor dynamics, the order analysis is preferred over the frequency spectrum analysis. In the order domain, the values of the fundamental order and the harmonics remain constant with respect to the shaft speed: first order is always at the shaft speed, second order is always twice shaft speed, and so on.

To achieve order analysis in rotating machinery applications, instead of sampling at equal increments of time, a different sampling technique has to be used: sampling at equal increments of rotation. This is called synchronous sampling. The synchronous sampling technique is very useful for rotating machinery related data processing, especially for those with varying shaft speed, but it is difficult to realize in practice.

Generally, there are two approaches to achieve the synchronous sampling—analog and digital approaches.

The analog approach uses an A/D sampling clock to achieve synchronous sampling. The key to this approach is to generate an appropriate sampling clock based on shaft rotation conditions. As shown in Fig. 4, the sampling clock is derived from the shaft tachometer by a ratio generator to meet the desired order analysis requirements (such as order resolution and maximum order). In cases where only lower order components are of interest, the tachometer output can be used as a sampling clock directly.

In the digital approach, both the vibration and the tachometer signals are discretized simultaneously, preferably at high speed. Different signal processing techniques can be used to resample the data and convert time domain data into shaft cycle domain data, with the help of a tachometer signal from the shaft. Nevertheless, the availability of the shaft tachometer/synchrophaser is crucial to both analog and digital synchronous sampling approaches.

With the synchronously sampled data, a common way to en-

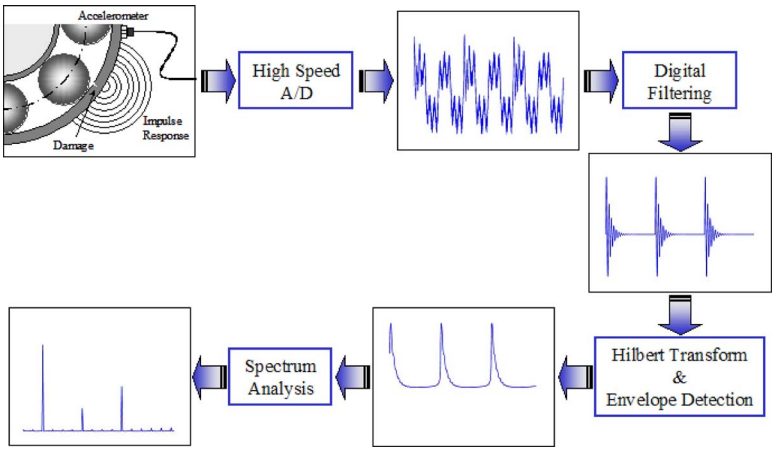

Fig. 3 Digital processing based approach

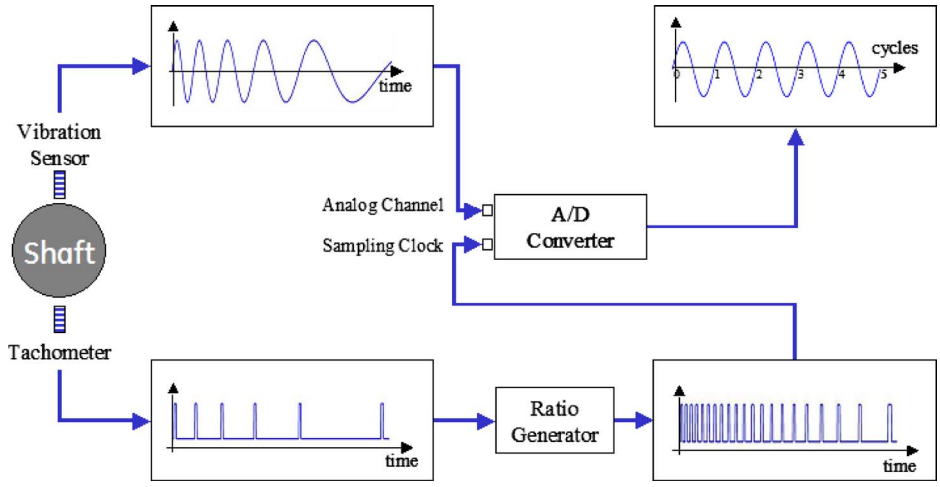

Fig. 4 Synchronous sampling—analog approach

hance the signal components of interest is through the time synchronous averaging [10]. With a shaft tachometer, the vibration signal detected contains three major components: the synchronous coherent signal component, the synchronous noncoherent component, and random noise. Conventional time synchronous averaging can only enhance the synchronous coherent signal component. The synchronous noncoherent component and random noise will be averaged out with sufficient number of averages.

Figure 5(*a*) shows a simulation result with a combination of the shaft response, $a\sin(2\pi f_0 t)$, its second harmonic $b\sin(4\pi f_0 t)$, a nonsynchronous coherent signal, $c\sin(2\pi\cdot 1.3\cdot f_0 t)$, and a uniform random noise. After 250 times of synchronous averaging, the results are shown in Fig. 5(*b*), where the random noise and nonsynchronous coherent component have been successfully removed.

When applying the synchronous sampling technique to the bearing damage detections, there are two problems that need to be resolved. The first is that the bearing damage signatures are usually nonsynchronous component to the shaft order, as seen in Eqs. (1)–(4). So, if the regular time domain synchronous averaging technique is applied to the vibration response, the bearing damage signatures will be averaged out. The second problem is unique to a differential bearing. In this case, both races are moving, and the damage frequencies are function of the race speed difference. However, it is physically impossible to have a tachometer that measures the rotational differential shaft speed. Digital signal processing is mandatory to achieve synchronous sampling. In the Sec. 3 we will introduce the synthesized synchronous sampling technique and demonstrate its feasibility with numerical simulations.

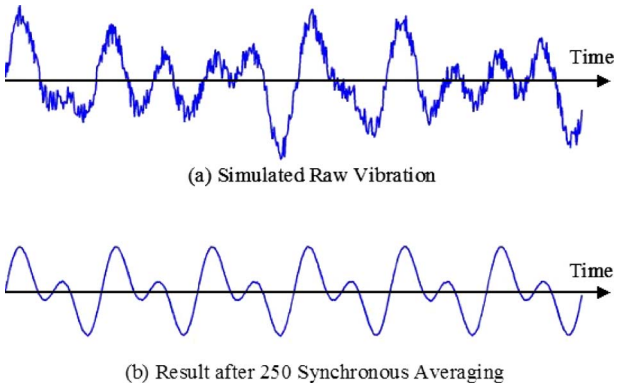

Fig. 5 Time synchronous averaging

3 Synthesized Synchronous Sampling

3.1 Fundamentals of Synthesized Synchronous Sampling. With the help of a tachometer, the equal time sampled data can be converted into equal shaft angular space data, as shown in Fig. 6.

In the event that the direct shaft tachometer signal is not available, traditional synchronized sampling becomes difficult, if not infeasible. For example, in some aircraft engines, the high-speed turbine shaft is not directly accessible to a tachometer. Its speed is deduced from the gearbox rotations, since it interfaces with the high-speed turbine shaft. However the gear ratio is not necessarily an integer. Thus, the shaft speed can be derived from counting the gear teeth and then multiplying by a noninteger constant. If a synthesized tachometer signal can be generated from the speed signal, then the equal circumferential space sampling (synchronous sampling) can then be carried out following well-established routines.

The following describes a procedure to synthesize a tachometer from the shaft speed profiles. Referring to Fig. 7, assume we have determined the synthesized tachometer generated a pulse at time t_i, we need to find out the location of the next pulse timing t_{i+1}. The time elapsed from t_i to t_{i+1}, i.e., $\Delta t_1 = t_{i+1} - t_i$, is the instantaneous shaft rotation period. On the other hand, if we have determined the t_{i+1}, since we know the shaft speed as a function of time, the average speed n between t_i and t_{i+1} can be calculated numerically. Therefore, the shaft instantaneous period can also be approximated by the averaged instantaneous shaft speed, i.e., $\Delta t_2 = 60/n$. In theory, by equalizing Δt_1 and Δt_2, we can determine t_{i+1}, thus calculating the next pulse location. In practice, due to time resolution and speed accuracy, an approximation procedure is used instead of exact solution. The following steps further explain the procedure of the synthesized synchrophaser:

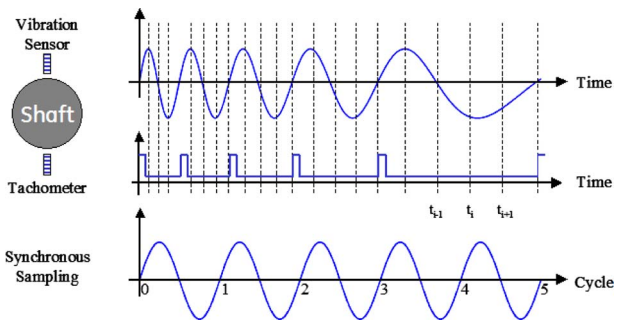

Fig. 6 Synchronous sampling

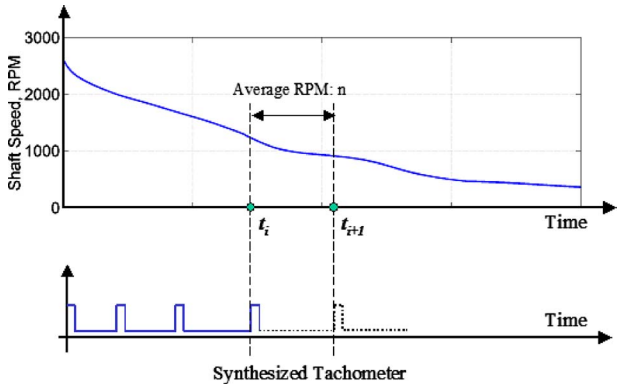

Fig. 7 Synthesized tachometer generation from speed function

1. Assume a synchrophaser pulse at time zero.
2. Once the ith synchrophaser pulse is located, at t_i, assume the $(i+1)$th pulse be located at t_{i+1}.
3. Calculating the average shaft speed n in RPM, which is a function of t_{i+1} from t_i to t_{i+1}

$$n(t_{i+1}) = \frac{1}{t_{i+1} - t_i} \int_{t_i}^{t_{i+1}} \text{Shaft speed}(t)dt \tag{6}$$

4. Formulate the time elapsed from t_i to t_{i+1}

$$\Delta t_1 = t_{i+1} - t_i \tag{7}$$

and the time elapsed by one instantaneous rotation

$$\Delta t_2 = 60/n \tag{8}$$

5. Solve t_{i+1} such that $|\Delta t_1 - \Delta t_2|$ is minimized.

t_{i+1} is then the approximate location of the $(i+1)$th synchrophaser pulse. The tachometer can be generated from the synchrophaser, say, by equal spacing between the consecutive synchrophaser pulses.

With this method, one of the major error sources is the discretization resolution. The maximum error in the shaft period is $T/2$, where T is the sampling period. Fortunately, for bearing and gear dynamic response analysis, especially the acceleration enveloping analysis, the frequency of interest is usually much higher than the shaft speed. In other words, the digitization rate is usually several orders of magnitude higher than the shaft speed. Thus, synthesizing error from the digitization error is expected to be negligibly small.

3.2 Simulations. To demonstrate the feasibility of the synthesized synchronous sampling method described in Sec. 3.1, numerical simulations were carried out. In the simulations, a shaft is assumed to be varying in speed from 240 rpm to 600 rpm in 4 s, following a half sine wave. The shaft speed as a function of time is plotted in the top portion of Fig. 8. The corresponding pulse train is simulated, as seen in the bottom portion of Fig. 8.

By using the shaft speed information and the procedures described in Sec. 3.1, we are able to generate a synthesized pulse train. As shown in Fig. 9, the synthesized pulse train (dashed line) is overlaid with the simulated pulse train (solid line). The synthesized pulse train has very similar frequency pattern as in the simulated pulse train. Their phase difference is expected, since we assumed a pulse at the time zero in the synthesized pulse train.

From the synthesized pulse train, we can derive the shaft speed. In Fig. 10, we have shown the shaft speed synthesized from the synthesized pulse train (dash-dotted line). The simulated "exact" solution is also plotted (solid line) for comparison. The difference between them is also shown as a dotted line. As seen from the figure, the synthesizing procedure is accurate for a perfectly simulated signal. To quantify the error, we have defined an error measure as

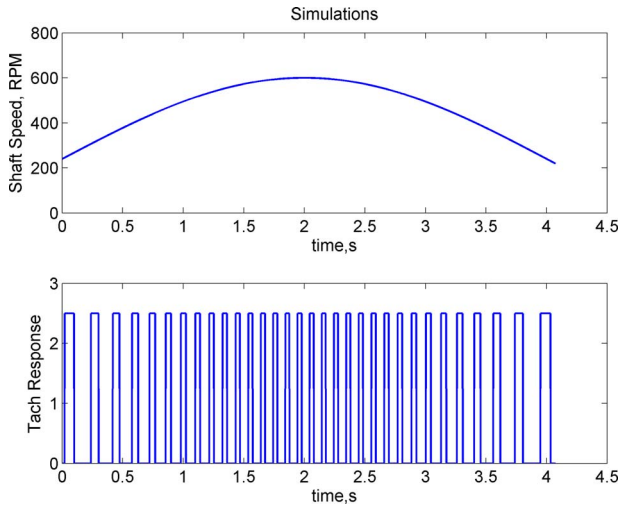

Fig. 8 Simulated varying shaft speed and the corresponding pulse train

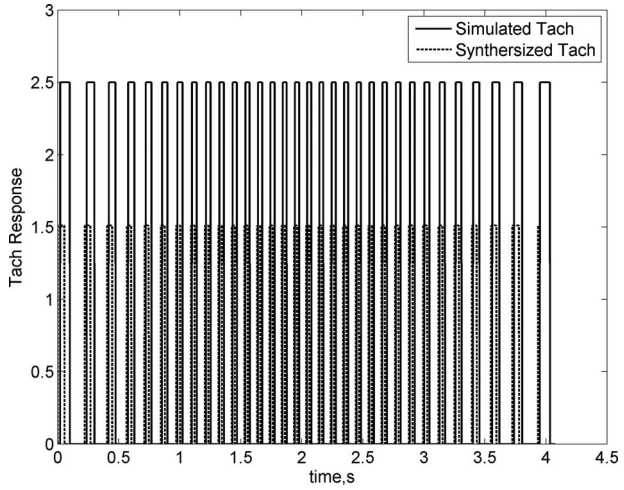

Fig. 9 Synthesized pulse train

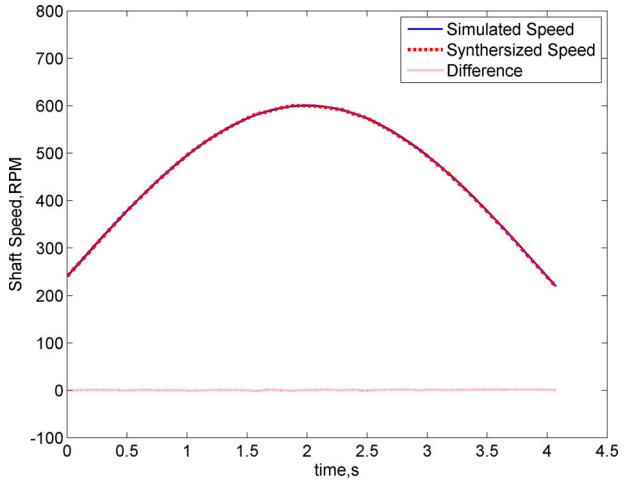

Fig. 10 Synthesized speed

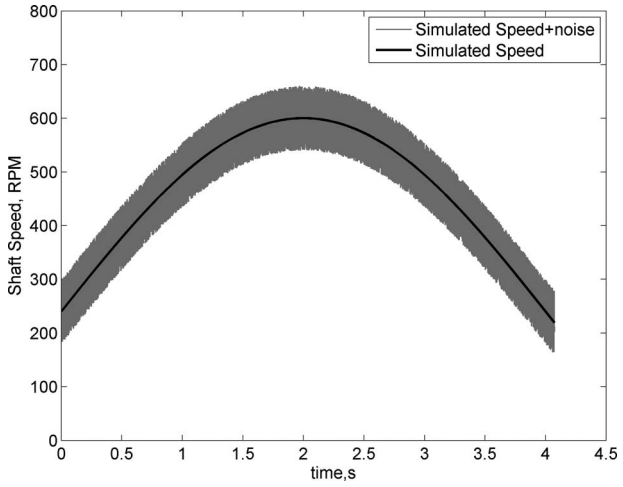

Fig. 11 Speed error simulation

$$\text{Error} \equiv \sqrt{\frac{(n_{\text{simulated}} - n_{\text{synthesized}})^T \cdot (n_{\text{simulated}} - n_{\text{synthesized}})}{n_{\text{simulated}}^T \cdot n_{\text{simulated}}}} \times 100\% \quad (9)$$

where $n_{\text{simulated}}$ is the simulated shaft speed, $n_{\text{synthesized}}$ is the synthesized shaft speed, and $(\bullet)^T$ is the vector transpose. Using this measure, the synthesizing error for the simulation signal above is less than 0.2%.

To investigate the robustness of the algorithm, the shaft speed was added with uniform noise to simulate the measurement error. As shown in Fig. 11, the simulated shaft speed (dark line) was added with uniform noise having 120 rpm peak-to-peak error. The synthesizing procedure still resulted in a satisfactory conclusion. The synthesized speed error measured by Eq. (9) is less than 1%. In Fig. 12, we have shown the synthesizing error for speed error up to 240 rpm peak-to-peak. All the synthesizing errors are within 3%.

Numerical simulations demonstrated that the proposed synthesizing procedure could accurately reproduce the tachometer pulse train for an accurate shaft speed input. It can also tolerate zero mean noise very well. By examining Eq. (6), it is evident that zero mean noise in the shaft speed can be averaged out in this step.

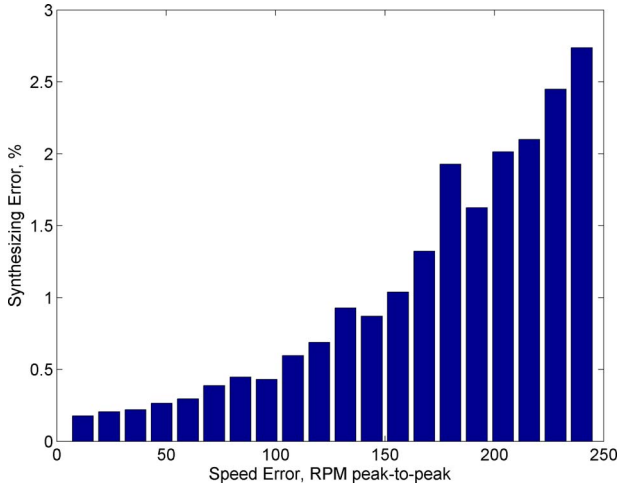

Fig. 12 Synthesizing error

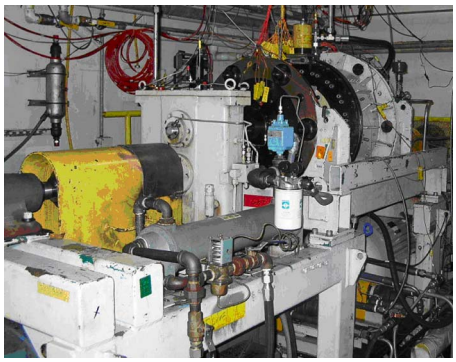

Fig. 13 Differential bearing test rig

4 Differential Bearing Damage Detection

4.1 Test Facility. An existing rig at the General Electric (GE) Aviation bearing laboratory (Evendale, OH) was modified to suit the differential bearing test, as shown in Fig. 13. The rig has the capability for periodic partial teardowns to inspect, photograph, and measure spalls generated in the differential bearing.

The fault simulation was determined by the customer requests to simulate an axial scratch from a roller scraping the outer race during a misaligned assembly. One of the seeded damages was an electric discharge machining (EDM) notch on the outer race surface, as shown in Fig. 14.

The test rig was instrumented with various sensors, including speed sensors, load cells, acoustic emission sensors, oil debris sensors, strain gauges, thermocouples, and accelerometers, etc. For the purpose of this research, we focused on the accelerometer and speed sensor data only. The schematic of the sensor location is shown in Fig. 15. The accelerometers used in the test have resonant frequency above 12 kHz to guarantee the information from high frequency response. Accelerometer data were sampled at 200 kHz.

4.2 Synthesized Synchronous Sampling Based Algorithm Implementation. We have implemented the synthesized synchronous sampling based on a differential bearing detection algorithm for this test. The major steps of the procedure are shown in Fig. 16.

1. Digitize the conditioned vibration sensor at high sampling frequency with high dynamic range A/D converter.
2. Apply a digital bandpass filter to the digitized vibration data to isolate the damage induced impulse response, by removing low frequency shaft responses and very high frequency noise.
3. Apply the Hilbert transform to the bandpass filtered data to detect the envelope of the signal.

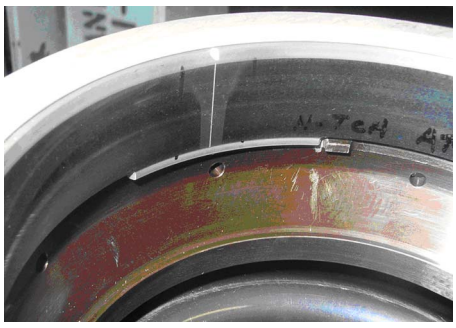

Fig. 14 Test bearing with EDM notch on the outer race

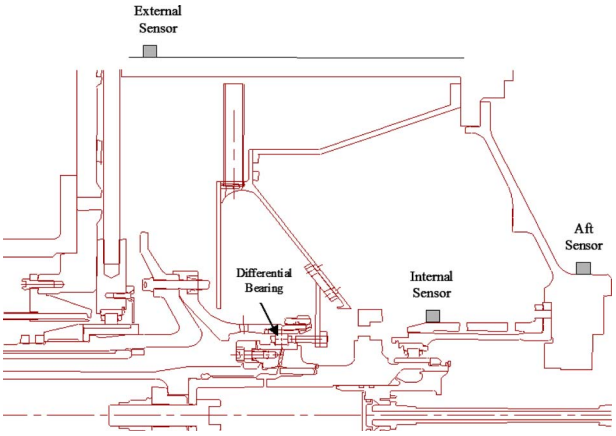

Fig. 15 Locations of accelerometer on the test rig

4. Digitize both the LPT and HPT shaft speeds simultaneously with the vibration data.
5. Derive the instantaneous speed difference from the speed signals.
6. Generate the synthesized synchrophaser pulses according to Sec. 3.
7. Generate synthesized tachometer based on order analysis requirements (i.e., maximum order and order resolution).
8. Carry out "synchronous sampling" to the envelope data derived in Step 3, which will convert the envelope in time domain into "synthesized" cycle domain.
9. Apply FFT onto the cycle domain data to get the order spectrum.
10. Average in order domain to further enhance the signature as needed.

The test case analyzed here had the outer race of the differential bearing embedded with an EDM groove, as shown in Fig. 14. A segment of the test data (approximately 10 s) was extracted for detailed analysis. In this period, the outer race speed changed significantly, while the inner race maintained approximately constant, as shown in Fig. 17. The corresponding ball (or roller) passing frequency outer race (f_{BPFO}) in frequency domain (Fig. 18) and the order number (O_{BPFO}) in the order domain were calculated according to Eq. (4).

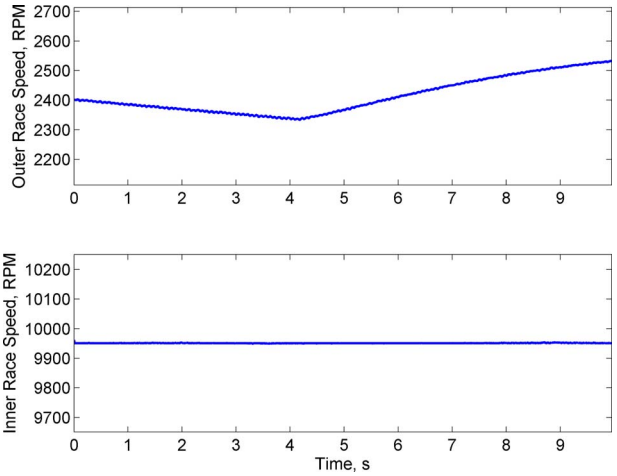

Fig. 17 Speeds of the differential bearing races

In the following analysis, the data from the external accelerometer (refer to Fig. 15) were used. A bandpass filter of 40–60 kHz was used for acceleration enveloping detection. Twenty averages were applied to both frequency and order spectra. Without the technique proposed here, it is almost impossible to identify any signature from a regular FFT spectrum of an accelerometer signal (Fig. 19(*a*)). With regular acceleration enveloping, we can barely see a small bump around the BPFO frequency location, as shown in Fig. 19(*b*). This is because both race speeds are not precisely controlled. A small drift in the race speeds is amplified at the bearing signature frequency. As a result, the bearing signature was smeared out in the neighborhood of the BPFO frequency and cannot be clearly identified. When the synthesized sampling technique was applied, the damage signature was then greatly enhanced, as seen in Fig. 19(*c*). Further examination of Fig. 19(*c*), we can see that the current process has enabled us to enhance the main damage signature f_{BPFO}. It has also brought out other features such as higher order harmonics of the main damage feature and sidebands around the main feature.

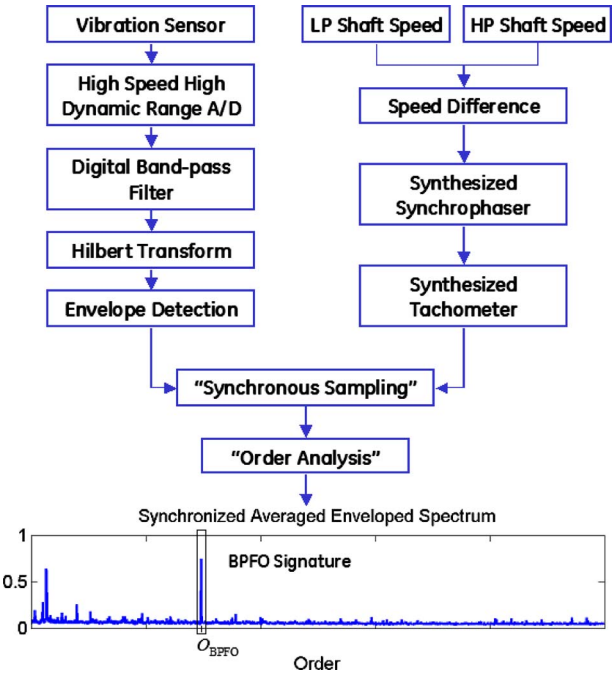

Fig. 16 Implementation flow chart

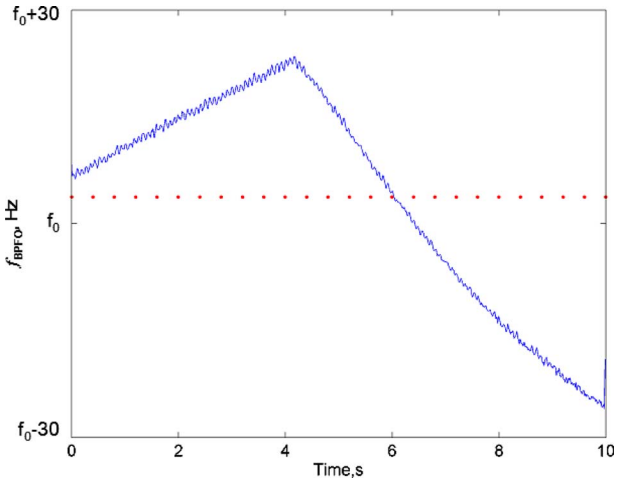

Fig. 18 Differential bearing f_{BPFO}

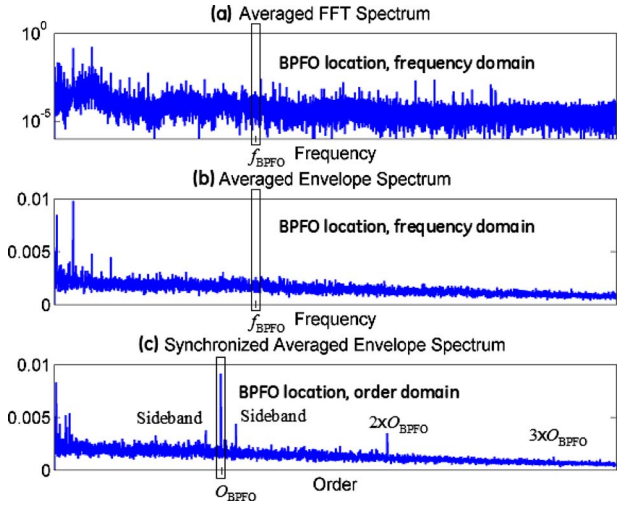

Fig. 19 Initial results

5 Conclusions

A procedure for the detection of differential bearing damage was developed and presented. The key for the differential bearing damage detection is the construction of a synthetic tachometer signal for the case of a bearing with both races moving. In such a case, a conventional tachometer is not physically feasible. The digital synthesizing technique provided in this paper confirmed the possibility for differential bearing damage detection using synchronous sampling technique. Together with the acceleration enveloping technique, the synthesized synchronous sampling technique has proven to greatly enhance the main damage signature as well as other features such as higher order harmonics and sidebands.

It also worth noting that with the development of computer technology and data processing techniques, those damage detection system functionalities traditionally achieved by analog components can be replaced by digital signal processing after high-speed and high-dynamic range A/D conversion. The benefits of digital processing are multifolds: it can improve the damage detection accuracy, sensitivity, and flexibility; it can also improve reliability by reducing the number of system components; and finally, it can reduce the damage detection cost by eliminating the analog components.

Acknowledgment

Part of the experimental data used in this paper was obtained from the work supported by the Defense Advanced Research Projects Agency, Defense Sciences Office (DSO), Engine System Prognosis, issued by DARPA/CMO under Contract No. HR0011-04-C-0002. The authors would appreciate suggestions and guidance given by DARPA red team members.

References

[1] McFadden, P. D., and Smith, J. D., 1984, "The Vibration Monitoring of Rolling Element Bearings by the High-Frequency Resonance Technique—A Review," Tribol. Int., **17**(1), pp. 3–10.
[2] Howard, I., 1994, "A Review of Rolling Element Bearing Vibration Detection, Diagnosis and Prognosis," DSTO Aeronautical and Maritime Research Laboratory, Melbourne, Australia, Paper No. DSTO-RR-0013.
[3] Rao, J. S., 2000, *Vibratory Condition Monitoring of Machines*, Narosa Publishing House, New Delhi.
[4] Eshleman, R., 2002, *Machinery Vibration Analysis: Diagnostics, Condition Evaluation, and Correction, Vibration Institute*, Vibration Institute, Clarendon Hills, IL.
[5] McFadden, P. D., and Smith, J. D., 1984, "Model for the Vibration Produced by a Single Point Defect in a Rolling Element Bearing," J. Sound Vib., **96**(1), pp. 69–82.
[6] McFadden, P. D., and Smith, J. D., 1985, "Model for the Vibration Produced by Multiple Point Defect in a Rolling Element Bearing," J. Sound Vib., **98**(2), pp. 263–273.
[7] Harker, R. G., and Sandy, J. L., 1989, "Rolling Element Bearing Monitoring and Diagnostics Techniques," ASME J. Eng. Gas Turbines Power, **111**, pp. 251–256.
[8] Su, Y. T., and Lin, S. J., 1992, "On Initial Fault Detection of a Tapered Roller Bearing: Frequency Domain Analysis," J. Sound Vib., **155**(1), pp. 75–84.
[9] Stewart, R. M., 1977, *Some Useful Data Analysis Techniques for Gear Box Diagnostics*, University of Southampton.
[10] Hochmann, D., and Sadok, M., 2004, "Theory of Synchronous Averaging," IEEE Aerospace Conference, Big Sky, MT.
[11] Combet, F., and Gelman, L., 2007, "An Automated Methodology for Performing Time Synchronous Averaging of a Gearbox Signal Without Speed Sensor," Mech. Syst. Signal Process., **21**(6), pp. 2590–2606.
[12] Darlow, M. S., Badgley, R. H., and Hogg, G. W., 1974, "Application of High-Frequency Resonance Techniques for Bearing Diagnostics in Helicopter Gearboxes," Paper No. ADA004014.
[13] Bogert, B. P., Healy, M. J. R., and Tukey, J. W., 1963, "The Frequency Analysis of Time Series for Echoes: Cepstrum, Pseudo-Autocovariance, Cross-Cepstrum, and Saphe Cracking," *Proceedings of the Symposium on Time Series Analysis*, M. Rosenblatt, ed., Wiley, New York, Chap. 15, pp. 209–243.
[14] Su, Y. T., Lin, M. H., and Lee, M. S., 1993, "The Effect of Surface Irregularities on Roller Bearing Vibrations," J. Sound Vib., **165**(3), pp. 455–466.
[15] Harting, D. R., 1978, "Demodulated Resonance Analysis—A Powerful Incipient Failure Detection Technique," ISA Trans., **17**, pp. 35–40.
[16] Frarey, J. L., 1996, "The History and Application of the Envelope Detector," Technology Showcase: Integrated Monitoring, Diagnostics and Failure Prevention, Proceedings of a Joint Conference, Mobile, AL.
[17] Broderick, J. J., Burchill, R. F., and Clark, H. L., 1972, "Design and Fabrication of Prototype System for Early Warning of Impending Bearing Failure," NASA Report Nos. MTI-71TR1 and NASA-CR-123717.
[18] Marple, S. L., Jr., 1999, "Computing the Discrete-Time Analytic Signal Via FFT," IEEE Trans. Signal Process., **47**(9), pp. 2600–2603.
[19] Luo, H., Fang, X., and Ertas, B., 2009, "Hilbert Transform and Its Engineering Applications," AIAA J., **47**(4), pp. 923–932.